AIMS Geosciences

https://www.aimspress.com/journal/geosciences/

AIMS Geosciences, 11(4): 885–906
DOI: 10.3934/geosci.2025038
Received: 13 March 2025
Revised: 17 June 2025
Accepted: 19 August 2025
Published: 27 October 2025

Research article

Permeability of coarse silts using dissipation tests in cone penetration test: Case study, Finninmäki testing site

Mohammad Sadegh Farhadi*, Eetu Pöyry and Tim Tapani Länsivaara

Research Center TERRA, TERRA-Geo group, Faculty of Built Environment, Tampere University, Korkeakoulunkatu 5, 33720 Tampere, Finland

* **Correspondence:** Email: mohammadsadegh.farhadi@tuni.fi; Tel: +358-50-433-3321.

Abstract: Dissipation tests were performed at the Finninmäki testing site, Tampere, Finland, through the cone penetration test (CPTu). In these tests, both contractive and dilative behaviors were observed. The parameter t_{50}, the time when 50% of initial pore pressure, u_2, dissipates, was computed for the tests using three methods proposed in literature. Then, soil permeability, k, was estimated following two approaches, using either t_{50}-based empirical equations or CPTu-based methods. It was observed that the t_{50} values interpreted from the three methods were considerably different. The differences in the estimated t_{50} values led to considerably variable k estimations approximated by the t_{50}-based empirical equations. On the other hand, the CPTu-based k estimates were considerably different from the t_{50}-based estimations. Besides, three undisturbed soil samples were taken by the 132 mm TUNI tube sampler in the field. These samples were used in the lab to measure the soil permeability, k, experimentally. Comparison of the experimental measurements with the k estimates highlighted the significance of the improvement required for the available empirical equations to estimate k for the studied coarse silts.

Keywords: silty testing site; cone penetration test (CPTu); dissipation test; laboratory permeability test

1. Introduction

The accurate multi-channel and continuous measurements of (piezo-)cone penetration test (CPTu) is the great advantage of this geotechnical field testing method. This advantage has made it a superior tool, which is beneficial in saturated varved fine-grained soils. It can provide much information on the physical and mechanical properties of soils, by interpreting its three major measurements: cone tip resistance, q_c, sleeve friction, f_s, and pore water pressure at the shoulder of the piezocone, u_2. These measurements are well correlated with several geotechnical properties, such as soil permeability, k [1], which is addressed in this study.

Among the three primary CPTu measurements, u_2 is recognized as the most rapidly responsive and sensitive to changes and variations in soil conditions. This sensitivity is particularly advantageous in dissipation testing, where u_2 is monitored over time after halting penetration at a specific depth, enabling estimation of soil permeability, k [2–4]. It should be noted that it is influenced by the degree of saturation in the piezocone's porous stone [5–7]. Parez and Fauriel (1988) studied the horizontal permeability, k_h, from CPTu dissipation tests. To simplify, parameter t_{50}, was used in their studies, which is interpreted from the u_2-time chart. It is defined as the time when 50% of the induced pore water pressure, u_2, is dissipated. A chart and an equation were proposed in their study to estimate k_h from the CPTu dissipation tests [2]. Ziaie-Moayed et al. (2009) optimized their equation to estimate k_h, for sandy soils [3]. In these studies, t_{50} was used as an indicative value of the whole u_2-time chart in the dissipation tests, which needs to be determined following a proper approach.

Parameter t_{50} can be interpreted differently for either contractive- or dilative-behavior u_2-time charts, and are also named standard and non-standard tests, respectively [4, 8]. The monotonic u_2-time contractive behavior can be interpreted straightforwardly to find t_{50}. However, for dilative behavior of soils, where the u_2-time chart appears as a piecewise convex-concave function, derivation of t_{50} can be more challenging, as discussed in different studies. For example, Sully et al. (1999) and Chai et al. (2012) proposed three methods to identify t_{50} from the dissipation tests for the dilative behavior [8, 9]. In the method proposed by Sully et al (1999), a higher u_2 is considered for its initial value, which is not actually measured in the test, but is determined from fitting a straight line to the post-peak concave part of the u_2-time chart. On the other hand, in the two methods proposed by Chai et al. (2012), the measured maximum u_2 is chosen as the highest initial u_2, and t_{50} is measured from that point. These methods are explained later in this paper.

In a different approach, several researchers addressed the determination of permeability, k, directly from the CPTu measurements. As an example, Robertson (2010) suggested two handy methods to estimate k [1]. These methods were proposed for all types of soils based on the soil index property, I_c, as presented in Eq. (1.1) [10].

$$I_c = \sqrt{((3.47 - logQ_{tn})^2 + (logF_r + 1.22)^2)} \tag{1.1}$$

where Q_{tn} and F_r, are the normalized CPTu parameters defined in [10,11], respectively, as $Q_{tn} = [(q_t - \sigma_{v0})/\sigma_{atm}](\sigma_{atm}/\sigma'_{v0})^n$ and $F_r = [f_s/(q_t - \sigma_{v0})]100\%$, where the exponent $n = 0.381I_c + 0.05(\sigma'_{v0}/\sigma_{atm}) - 0.15 \leq 1.0$ is iteratively calculated, after the first trial with $n = 1$, q_t is the corrected cone tip resistance, q_c, and f_s is the measured sleeve friction. More information on these interpreted parameters can be found in [10, 12].

The two CPTu-based k estimation methods proposed by Robertson (2010) [1] use either I_c directly in an empirical equation, or an interpretation of soil behavior type (SBT), using I_c as input. The two methods result in a deterministic value of k or a non-deterministic probable span of k values, respectively. Hereafter, they are called *empirical equation* and *SBT-based estimation* methods.

In this study, the aforementioned methods have been evaluated to determine permeability, k, for a silty testing site in Finland, following either dissipation-based or CPTu-based approaches. As a case study, a varved coarse silty soil was investigated in project FINCONE II, at the Research Center TERRA, Tampere University (TAU), Finland. In the next section, the testing site is described. The investigation was performed by means of CPTu test, seismic CPTu (SCPTu), CPTu dissipation tests, and the lab permeability and particle size grading tests. The tests performed in the field and the lab

are presented later in the third section. Thereafter, the methods to find permeability, k, are explained in detail. Finally, the estimated k values from the two dissipation-based and CPTu-based approaches are compared with the lab measurements, for both the contractive- and dilative-behavior dissipation tests.

2. Testing site

This paper reports a part of a comprehensive soil investigation carried out at a silty testing site, in the Finninmäki neighborhood, Tampere, Finland. After a preliminary field test, using CPTu and weight sounding tests, a smaller $6 \times 6\ m^2$ area was chosen to perform the tests. The location of the testing site is illustrated in Figure 1, which is at a small hillside. A very stiff layer was found at about 6.30 m deep, and no further tests were conducted deeper.

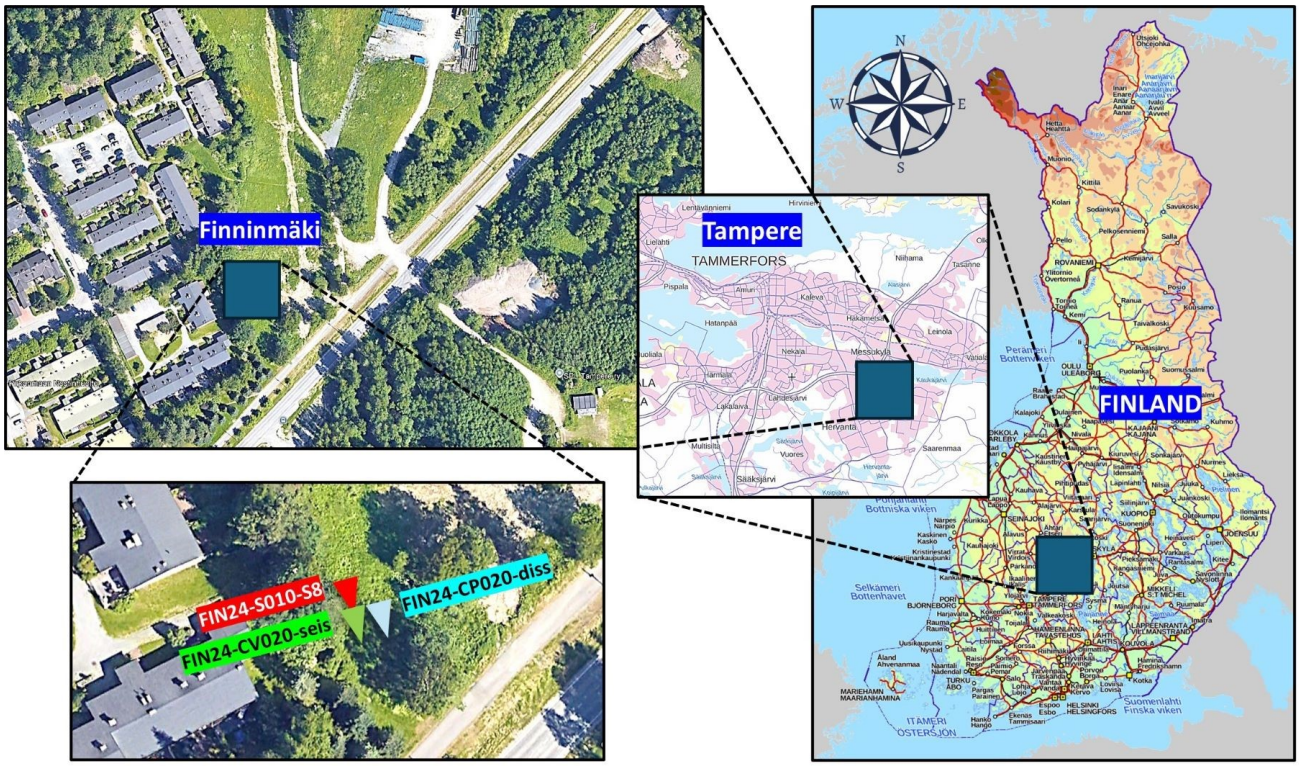

Figure 1. The location of the Finninmäki testing site, Tampere, Finland [13, 14]. The distances between the testing spots are approximately 2 m. The testing spots marked as FIN24-S010-S8, FIN24-CP020-diss, and FIN24-CV020-seis show the sampling, dissipation, and seismic CPTu tests spots, respectively.

3. Field testing

The field study reported here included soil sampling and CPTu testing, as described below.

3.1. Soil sampling

Three soil samples were taken to measure soil properties in the lab. The length of each cylindrical sample was about 500 mm and its diameter was 132 mm. The samples were taken using the TUNI sampler, which was developed at the Research Center TERRA, TAU. It was designed in the research project FINCONE I mainly to take high-quality sensitive clay samples. In this study, lubricant gel was used inside and outside the sampler to reduce the friction between the soil and sampler and to facilitate the intrusion of soil into the sampler. No sample catcher was used at the tip of the sampler tube to protect samples from falling off the tube during sample withdrawal. Instead, the inner surface of the sampler's cutting shoe was covered by one-directionally frictional fibers mainly to keep the loose samples from dropping out of the sampler. Details of the designed sampler with its technical specifications will be published in forthcoming reports of the study.

It worth mentioning that the Φ132 mm TUNI sampler and the lubricant led to no soil plug at the tip of the sampler, which was reported by Pöyry et al. (2024) for the Φ50 mm popular piston samplers in Finland, studied at the same testing site [15].

The test spot for the sampling borehole is denoted as "FIN24-S010-S8". The naming elements of the test spot ID, broken into "FIN", "24", "S", "010", and "S8" refer to the name of the testing site, "Finninmäki", year of action, "2024", purpose of the test spot, "Sampling", test number for the purpose, "010", and a code representing the sampler type, "S8: TUNI sampler with friction fibers", respectively. Such naming elements for different tests are presented in Table 1 as examples for different field tests, samples, and lab specimens.

Table 1. Examples to explain the information encrypted in the field and lab tests IDs.

ID	Purpose	Tool type	Test number	Sampler	Depth	Target test
FIN24-S010-S8*	Sampling		010	S8		
FIN24-CP020-diss	CPTu	P	020			Dissipation
FIN24-CV020-seis	CPTu	V	021			Seismic
FIN24-S010-S8-3.42-PSD	Sampling		010	S8	3.42	PSD**

* "FIN24", repeated in all IDs, stands for the name of the testing site and the year of action, meaning the testing site 'Finninmäki', and the actions performed in 2024.
** "PSD", stands for particle size distribution/grading test.

3.2. CPTu

The main CPTu test discussed in the paper is denoted as "FIN24-CP020-diss". As mentioned in its ID, this has been a CPTu test performed in conjunction with dissipation tests. The dissipation tests were performed at depths of 2.13, 2.70, 3.38, 4.39, 5.38, and 6.28 m, which were the same depths that the pushing rods were added during the piezocone penetration process. In this way, it was attempted to avoid further interruptions in the CPTu measurements.

The dissipation tests were performed after a deep enough penetration distance of the piezocone from the previous stop, or in other words, from the previous dissipation test, enabling excess pore pressure, u_2, to be induced after steady penetration of the cone at a constant rate of 20 mm/s [16]. Mainly in coarse-grained soils, halting the piezocone penetration affects the CPTu measurements,

specifically u_2 measurements, which occurs rapidly [17–19]. The penetration stoppage influence for CPTu measurements can be observed in Figure 2 for the studied Finninmäki testing site for test FIN24-CP020-diss. After each penetration stop, it may take a while, with penetration in depth, for the measurements to reestablish under constant rate of penetration. To avoid such interruptions in u_2 measurements in dissipation tests, the distances between the depth of dissipation tests were considered sufficiently far from each other. The shortest distance between two subsequent dissipation tests was from 2.13 to 2.70 m deep, equal to 57 cm distance. After positioning the piezocone at the desired depth, the u_2 variation was recorded with time until u_2 was dissipated almost completely, approaching the hydrostatic pore water pressure.

The raw measurements of the CPTu along with the interpreted soil index parameter, I_c, (eq. (1.1)), are illustrated in Figure 2. According to the study by Robertson (2016), the soils are mostly in $2.05 < I_c < 2.95$, which means that the soils in the testing site are sandy and silty mixtures [20].

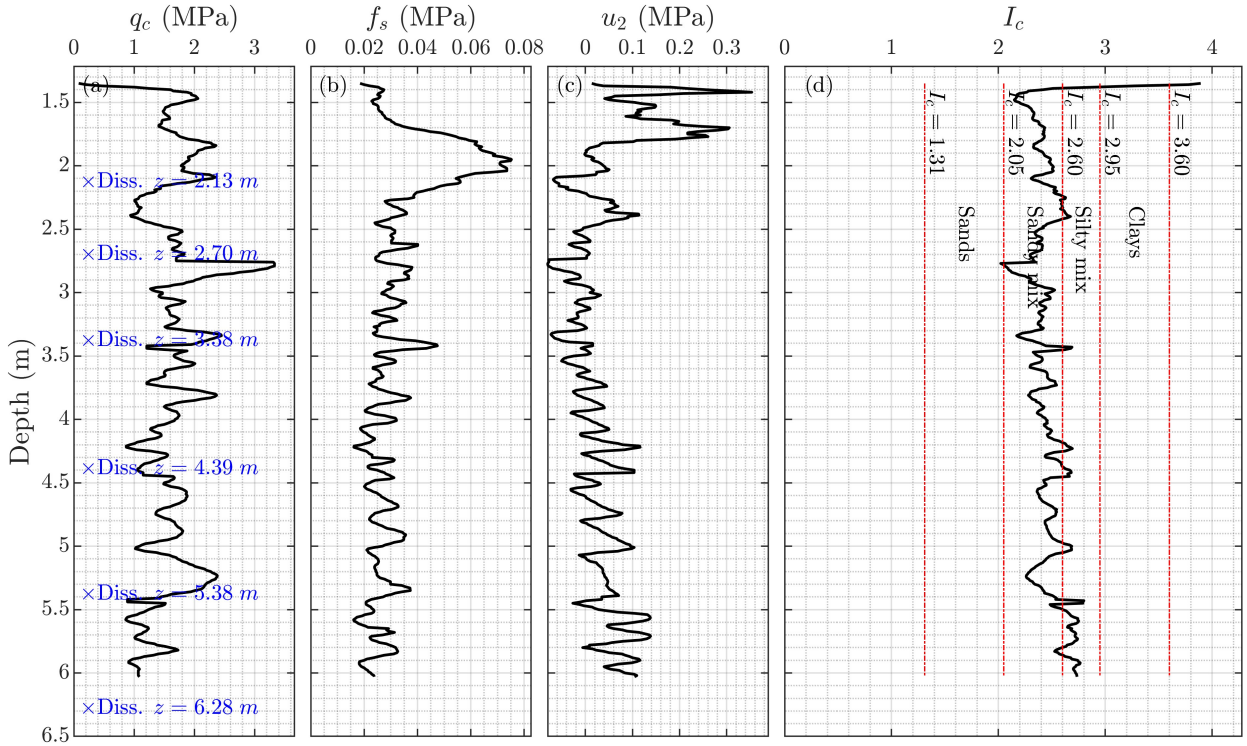

Figure 2. Raw piezocone measurements for the FIN24-CP020-diss test are shown in (a-c). The chart (d) shows the interpreted soil index I_c, proposed in eq. (1.1) [10]. The dashed lines for I_c=1.31, 2.05, 2.60, 2.95, and 3.60 are illustrated in chart (d) to differentiate the soil behavior types (SBTs) [10].

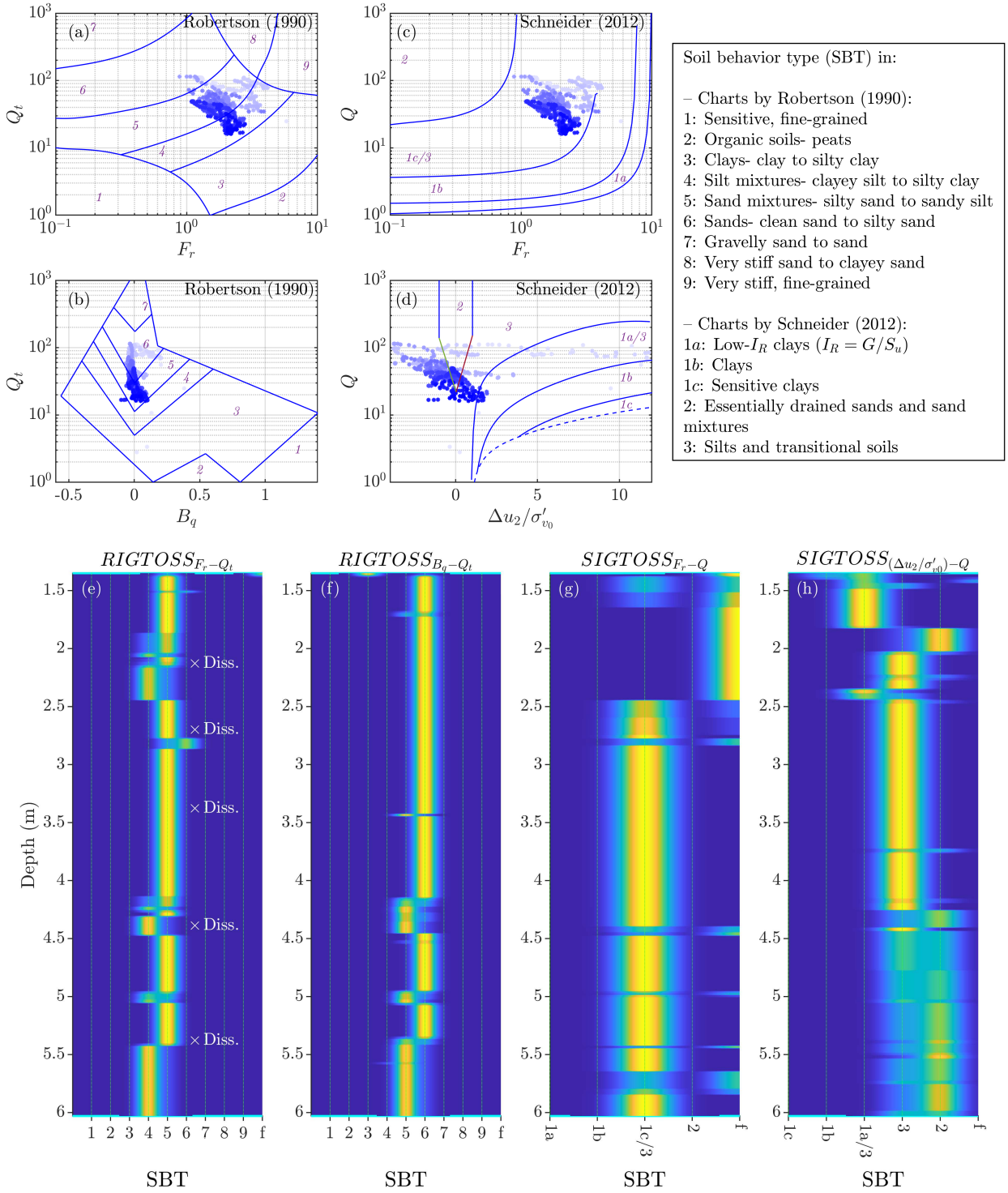

Figure 3. Distribution of the measurement points on the SBT characterization charts (a-d) are presented with the the stratification profiles by the -IGTOSS model (e-h) for FIN24-CP020-diss. The points on the characterization charts get darker with depth. The depths of the dissipation tests are marked in profile (e), except, the dissipation test at 6.28 m. More information on the -IGTOSS stratification model can be found in [21–23].

To ensure the accuracy of the u_2 measurements, the porous stone of the cone was saturated with glycerin oil, under vacuum, for 15–30 minutes. After saturation, it was stored fully submerged in the oil for an extended period, exceeding one year. During assembly, the porous stone and cone tip were carefully positioned so that the stone, cone, and pore pressure sensor chamber remained immersed in glycerin oil for several hours to effectively eliminate any air entrapment in the u_2 sensor.

The stratification profiles were derived using the FIN24-CP020-diss test results by means of the characterization-stratification -IGTOSS model [21–23]. The profiles are illustrated in Figure 3. The RIGTOSS$_{F_r-Q_t}$, SIGTOSS$_{F_r-Q}$, and SIGTOSS$_{\frac{\Delta u_2}{\sigma'_{v0}}-Q}$ models show mainly silt mixtures for the depth, i.e., soil behavior types (SBTs) of 4 and 5 for RIGTOSS$_{F_r-Q_t}$, and SBT of 3 for SIGTOSS$_{F_r-Q}$, and SIGTOSS$_{\frac{\Delta u_2}{\sigma'_{v0}}-Q}$ profiles. The RIGTOSS$_{F_r-Q_t}$ profile shows SBT of 5, indicating "sand mixutres-clayey silt to silty clay" at about 2.40-5.40 m. It is a bit different from the RIGTOSS$_{B_q-Q_t}$ results, which shows several layers with the SBTs of 6 and 5. These SBTs represent "Sands, clean sand to silty sand" and "Sand mixtures-silty sand to sandy silt", respectively.

The shear modulus, G, was calculated from the seismic CPTu (SCPTu) test, FIN24-CV020-seis, performed at a spot 2 m from the sampling point FIN24-S010-S8 and 2 m from the dissipation tests spot FIN24-CP020-diss. This proximity contributed to the comparability of the adjoining testing spots results to be used in the interpretations. The SCPTu test was performed by a piezocone, simply called "V" here, manufactured by a different company from the "P" piezocone, which was utilized for the dissipation tests.

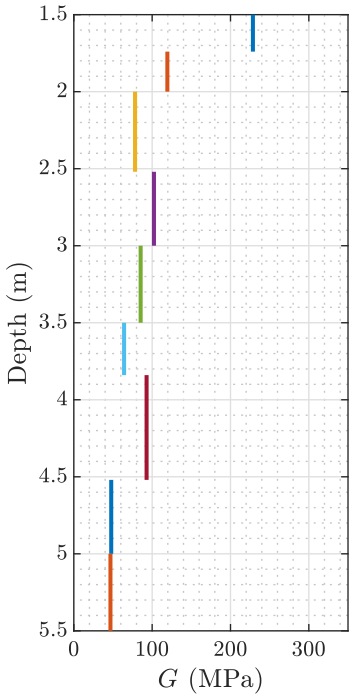

Figure 4. Shear modulus, G, obtained at different depth intervals in the seismic CPTu (SCPTu) test, FIN24-CV020-seis. Different colors are used to differentiate the results at the adjacent depths intervals.

The seismic tests were carried out at depth intervals of 25 or 50 cm, approximately. The specific

depths tested were 1.50, 1.74, 2.00, 2.52, 3.00, 3.50, 3.84, 4.52, 5.00, and 5.50 m, as illustrated in Figure 4. The shear modulus, $G = \rho V_s^2$, was computed using the average shear wave velocity, V_s, obtained from the hammer strikes on the base beam, from left and right sides. V_s was calculated based on travel time difference of waves between the succeeding testing depths. The soil density, ρ, was determined based on averaging the unit weight, γ, calculated using three empirical equations, two CPTu-based and one SCPTu-based, as presented in equations (4) and (7) in [24] and equation (3) in [1].

In this study, the shear modulus, G, was used in equation 5.1. The specifics of the seismic tests fall outside the scope of this study and will be addressed in a forthcoming publication.

4. Lab testing

Particle size grading and permeability tests reported in this study were performed for the three samples taken from the testing site.

4.1. Particle size grading

The particles size distribution (PSD) charts were measured from the hydrometer tests and sieve analysis, performed according to the standard ISO 17892–4:2016. The PSD results for three depths are illustrated in Figure 5. These PSD charts were measured using the trimming leftover soils of the permeability tests specimens described in the next section. The PSD chart at z = 3.28–3.40 m shows larger grains of soil compared to the other two PSD curves. This observation is consistent with the characterization results by RIGTOSS$_{F_r-Q_t}$, as shown in Figure 3-a.

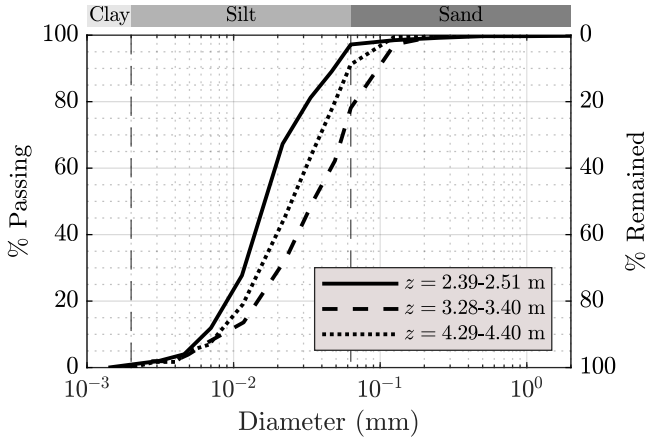

Figure 5. Particle size distribution (PSD) charts for the tests performed at different depths.

4.2. Permeability test

The lab permeability tests were performed under the in-situ isotropic mean effective stress in the triaxial setup. The back pressure was applied to make the required hydraulic gradient for the distilled water to flow through the sample. Three specimens were tested to measure the vertical permeability, k_v. The specimens were from depths of 2.39–2.50, 3.29–3.40, and 4.29–4.40 m. The large Φ132 mm diameter samples were trimmed using cutting wire and lathe in the lab to make the Φ50 mm specimens

for the permeability tests. In this process, it was observed visually that the soils from the testing site were noticeably varved.

The details of the conducted permeability tests and the corresponding vertical permeability values, k_v, for each test, are presented later in Table 3.

5. Results

The dissipation test results are presented in this section first, showing contractive- and dilative-behavior types of u_2-time charts. Several handy methods were applied to find k from these measurements, following two dissipation-based and CPTu-based approaches. Thereafter, the results of the lab permeability tests are presented.

5.1. Dissipation tests

The dissipation test results from FIN24–CP020-diss are illustrated in Figure 6, excluding the test conducted at 6.28 m. Each row in the figure corresponds to a distinct dissipation test. Acknowledging the CPTu influence zone during penetration, as outlined for example in [17], the figure includes ±5 cm spans of q_c, f_s, u_2, and the I_c to illustrate the uncertainties and variations in CPTu measurements near the dissipation test depths. Gaussian probability density functions (PDFs), $\mathcal{N}(\mu, \sigma)$, fitted to these intervals, are shown above each parameter, indicating their mean values, as well as μ. Additionally, CPTu measurements at the exact depths dissipation test depths are presented in the ±5 cm span charts.

Two types of u_2-time dissipation behaviors can be seen in Figure 6. They indicate the contractive and dilative deformation behaviors of soil, denoted as "standard" and "non-standard" behaviors [4, 25]. The contractive behavior in dissipation is observed at depths of 4.39 and 5.38 m. The dilative behavior in dissipation is observed for the other tests, at depths of 2.13, 2.70, 3.38, and 6.28 m.

5.2. Interpretation of dissipation tests for t_{50}

To interpret the dissipation tests results, t_{50} is commonly used for contractive behavior. The results for the two contractive dissipation tests are illustrated in Figure 7.

However, finding t_{50} for the dilative behavior can be challenging. For this purpose, in this study, three approaches were utilized.

Method 1: The first applied method was proposed by Sully et al. (1999) [8], and the other two methods were proposed by Chai et al. (2012) [9].

In the interpretation method by Sully et al. (1999), a straight line is fitted to the post-peak linear section of the u_2- $\sqrt{time}$ chart. Then, u_{max} is computed for the fitted line where it coincides with the u_2 axis at $t = 0$, and t_{50} is determined as the time when 50% of the u_{max} is dissipated. The interpretation results of the dilative-behavior dissipation tests are presented in Figure 8. This method is regarded as the *first* dissipation-based method assessed in this study for dilative-behavior tests.

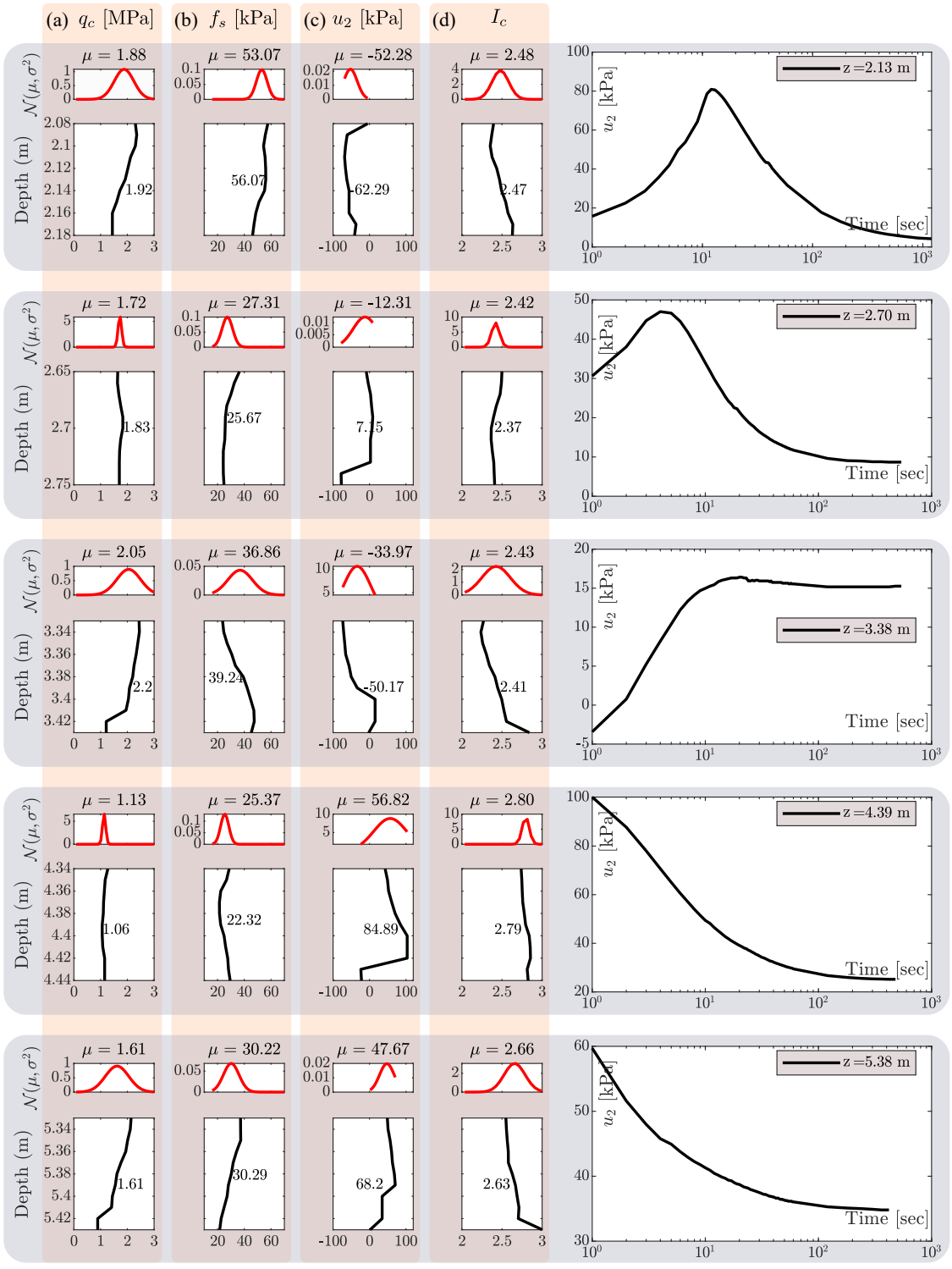

Figure 6. Dissipation tests results with the ±5 cm span of the CPTu measurements: (a) q_c, (b) f_s, (c) u_2, and (d) the calculated I_c. The dissipation test at 6.28 m is not illustrated while the proper CPTu measurements are not available, as an ending point of the CPTu test, just above the hard impenetrable layer.

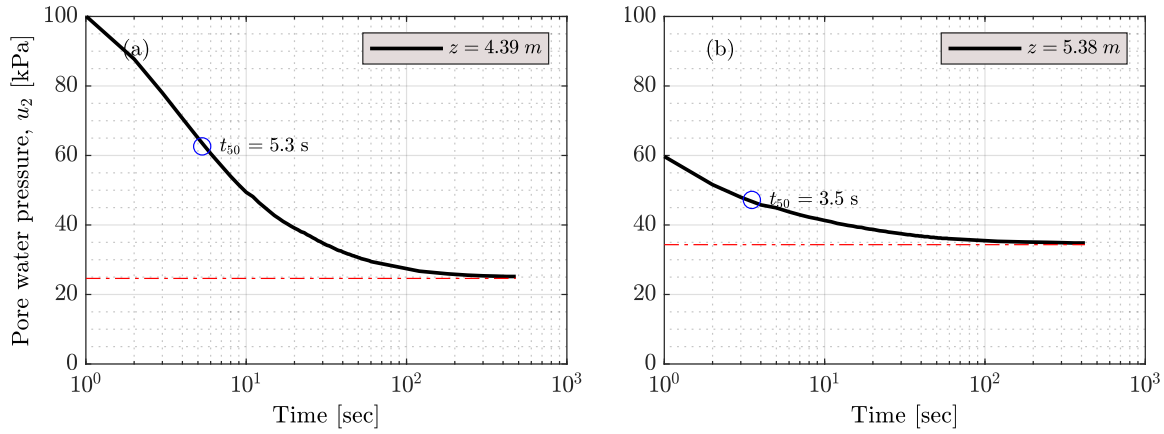

Figure 7. Calculated t_{50} for the two contractive-behavior dissipation tests.

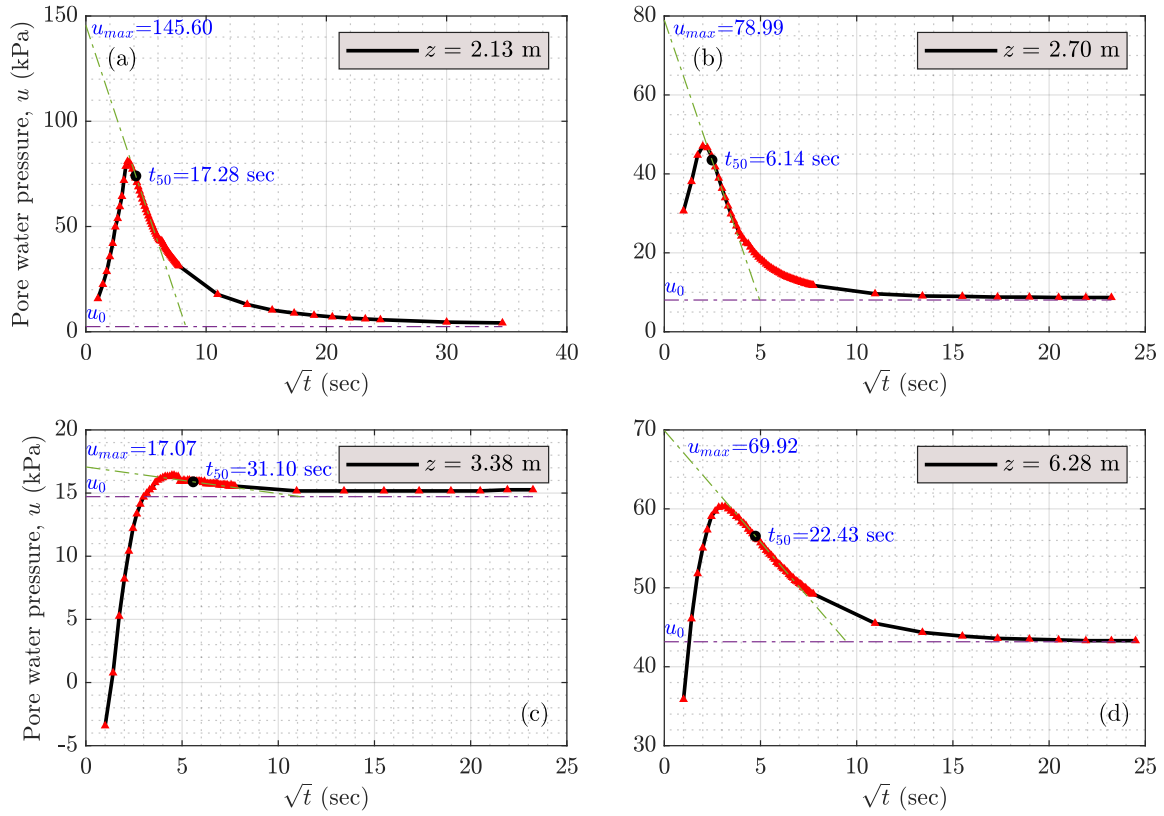

Figure 8. t_{50} interpreted after the first dissipation-based method, proposed by Sully et al. (1999) [8], for the dilative-behavior dissipation tests at different depths.

Method 2: As the *second* dissipation-based interpretation method, the one proposed by Chai et al. (2012) was utilized to determine t_{50} [9]. In this method, the dissipation u_2-time curve was cut from its peak, u_{max}, point. Then, the chart was plotted between the hydrostatic pore water pressure and the maximum measured u_2, normalized into [0 2] on the u_2 axis, $u_{2,norm}$. t_{50} was determined at $u_{2,norm} = 1$.

In other words, the initial (convex-)concave ascending part of the u_2-time curve was neglected, and t_{50} was measured from the u_{max} point. The t_{50} interpretation results from this method are illustrated in Figure 9 for the dilative behavior dissipation tests. As can be observed, the t_{50} values for z = 2.13, 2.70, 3.38, and 6.28 m are 29.51, 9.49, 34.03, and 32.92 seconds, respectively. The dissipation curve for z = 3.38 m appears unusual, displaying a nearly step-like pattern. This behavior results from the small variation in the post-peak u_2 measurements, which are normalized over a narrow pressure range. Consequently, the normalized data appear as discrete steps along the logarithmic time axis.

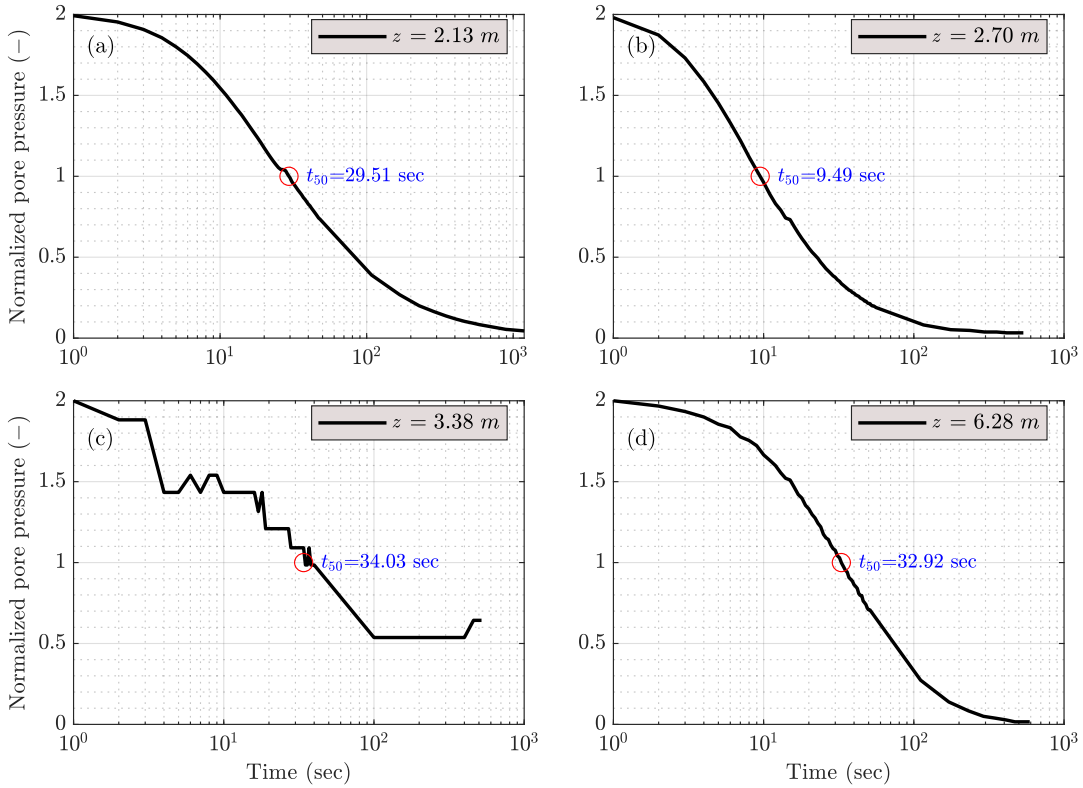

Figure 9. t_{50} interpreted after the second dissipation-based method, proposed by Chai et al. (2012) [9], for the dilative-behavior dissipation tests at different depths. No correction for the undrained shear strength, s_u, is applied in this method.

Method 3: As the *third* dissipation-based interpretation method, the previous method was followed, but the final t_{50} was corrected using the following equation [9]:

$$t_{50c} = \frac{t_{50}}{1 + 18.5(\frac{t_{u_{max}}}{t_{50}})^{0.67}(\frac{I_r}{200})^{0.3}} \tag{5.1}$$

where, t_{50c} is the corrected t_{50}, $t_{u_{max}}$ is the time of the maximum u_2, $I_r = G/s_u$ is the rigidity index, G is the shear modulus, and s_u is the undrained shear strength. The values of G used in the computations are illustrated in Figure 4, which were measured by the SCPTu test, at FIN24–CV020-seis. The s_u values in this equation were estimated based on two studies by Fu et al. (2024) [26] and Robertson & Cabal (2022) [12], following these two equations:

$$s_u = \frac{q_t - \sigma_v}{N_{kt}} \tag{5.2}$$

$$s_u = \frac{q_t - u_2}{N_{ke}} \tag{5.3}$$

where, for the N_{kt} and N_{ke}, the following values and equations were used:

1. $N_{kt} = 14$, as a typical average value, proposed by Robertson and Cabal (2022) [12],
2. $N_{kt} = exp(6.41424 - 1.489I_c)$, $1.8 \leq I_c \leq 2.8$, proposed by Fu et al. (2024) [26],
3. $N_{ke} = exp(6.31207 - 1.435I_c)$, $1.8 \leq I_c \leq 2.8$, proposed by Fu et al. (2024) [26].

where, s_u, q_t, σ_v, N_{kt}, N_{ke}, and I_c represent undrained shear strength, corrected cone tip resistance, vertical total stress, cone factor based on q_t, cone factor based on u_2, and the CPTu soil behavior type (SBT) index, respectively, proposed in [10]. The vertical total stress, σ_v, was calculated using the unit weight, γ, equation by Mayne et al. (2010) [24], as:

$$\gamma_t(kN/m^3) = 11.46 + 0.33log(z) + 3.10log(f_s) + 0.70log(q_t) \tag{5.4}$$

where, q_t and f_s are in kPa and depth, respectively, and z, is in meters.

Based on the mentioned equations, t_{50c} derived from different methods are presented in Figure 10. They are compared with t_{50}, which was the t_{50} before correction. The results are not presented for the dilative behavior test at 6.28 m tests as the CPTu test results are not available at that depth.

Table 2. Interpreted t_{50} for contractive- and dilative-behavior dissipation tests. t_{50} for dilative-behavior tests are interpreted by three methods explained in section 5.2.

Depth	Behavior		Method 1*	Method 2	Method 3			$\frac{(t_{50_{max}} - t_{50_{min}})}{t_{50_{max}}}\%$
					eq. (5.2)** [26]	eq. (5.3) [26]	eq. (5.2) [12]	
2.13	Dilative		17.28	29.51	1.79	1.80	1.84	93.9
2.70	Dilative		6.14	9.49	0.49	0.49	0.52	94.8
3.38	Dilative		31.10	34.03	1.65	1.66	1.74	95.1
4.39	Contractive	5.30						–
5.38	Contractive	3.50						–
6.28	Dilative		22.43	32.92				31.9

* Methods 1, 2, and 3 represent the the dissipation-based methods to find t_{50} proposed by Sully et al. (1999) [8], Chai et al. (2012) [9] without correction, and Chai et al. (2012) [9] with correction, respectively.

** For the correction of t_{50} in method 3, two values of N_{kt} and a single value of N_{ke} are used in equations 5.2 and 5.3, as explained after equation 5.3.

Figure 10 shows that the third method leads to much smaller values of t_{50c} after the correction through eq. (5.1). For example, Figure 10-a shows that t_{50c} is over 90% smaller than t_{50} at 2.13 m. t_{50}

is 29.51 s, derived from the second method, and after correction, t_{50c} is 1.84, 1.80, and 1.79 s, measured using two Eqs. (5.2) and (5.3), and the average value of N_{kt} proposed in [12] and N_{kt} [26] and N_{ke} [26], respectively.

To facilitate the comparison, the interpreted values of t_{50} in the dissipation-based approach are summarized in Table 2. The results are presented for both contractive- and dilative-behavior methods. Variations among the interpreted t_{50} values from different methods are compared with the maximum interpreted t_{50} for each dissipation test, by $100 \times (t_{50_{max}} - t_{50_{min}})/t_{50_{max}}$. Accordingly, the minimum and maximum variations are 31.9 and 95.1%, respectively, for all dilative tests. These results reveal that different methods lead to highly variable t_{50} interpretations in percentage. However, it should be noted that the interpreted t_{50} for the tests are not large numbers.

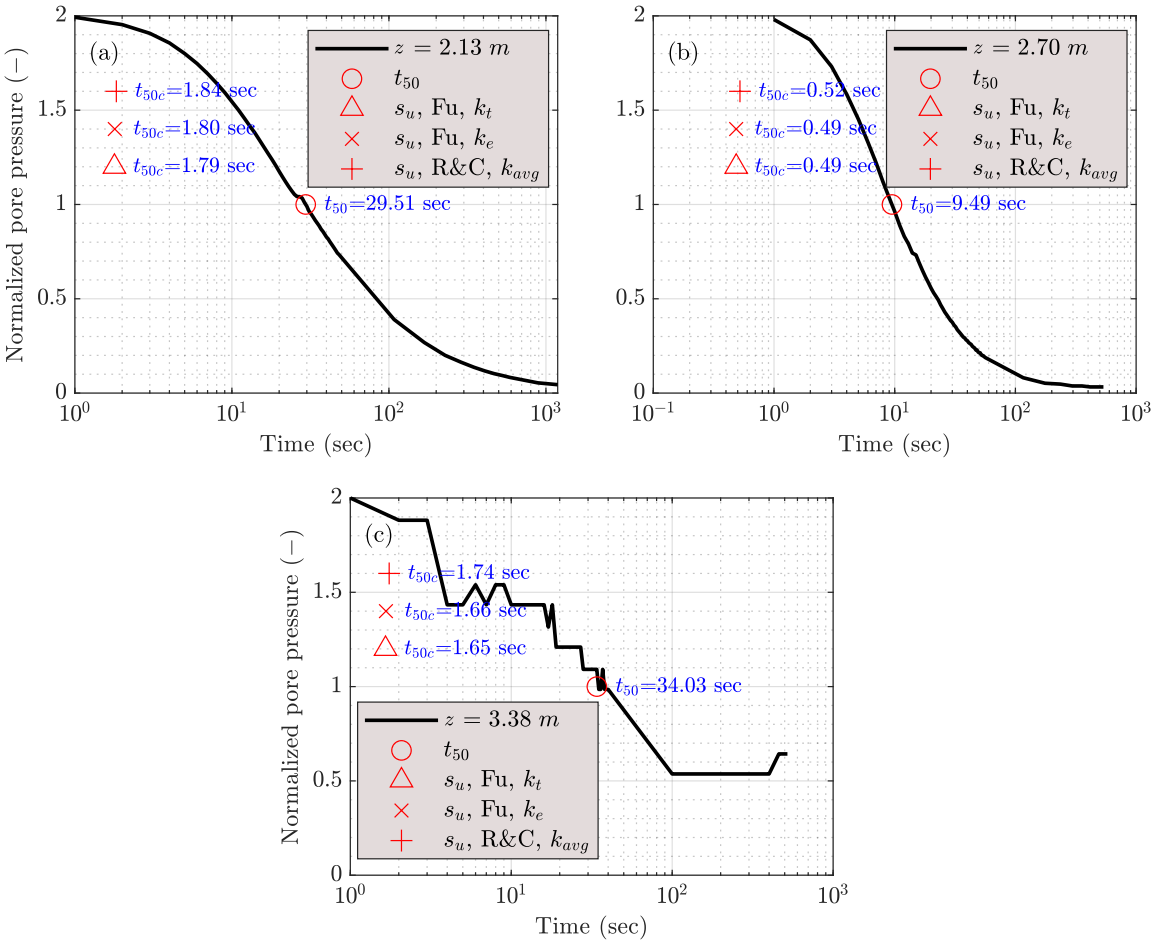

Figure 10. t_{50c} interpreted after the third dissipation-based approach, proposed by Chai et al. (2012) [9], for the dilative-behavior dissipation tests at different depths. The corrected t_{50c} are calculated using eq. (5.1). In this equation, s_u are estimated based on the equations proposed by Fu et al. (2024) [26], eqs. (5.2) and (5.3), and the average cone factor, $N_{kt_{avg}} = 14$, by Robertson and Cabal (2022) [12], used in eq. (5.2). For readability, the t_{50c} values at $u = 1$ are illustrated on the top of each other.

5.3. Permeability results

Three permeability tests were performed using undisturbed samples taken at the borehole FIN24–S8–S010. The permeability specimens were vertically trimmed out of the large samples, 50 mm in diameter and 110 mm in height. Table 3 presents the vertical permeability, k_v, measured for the three specimens. It is observed that the average k_v for the three specimens is 8.67E–7 m/s. The smallest k_v is observed for the sample at 3.29–3.40 m depth, where the largest sizes were measured (Figure 5). This can be due to the varved soil composition, which affects the k_v results.

5.4. Estimation of permeability, k

A goal for dissipation tests can be to estimate the permeability of soils, k. However, it is observed that the interpretation results of dissipation tests may be variable for parameter t_{50}, as a simplistic indicative of the whole dissipation test (Table 2). The impact of these interpreted t_{50} variations on the estimation of k were assessed for a varved coarse silty testing site, Finninmäki, Tampere, Finland. For this purpose, four handy methods were applied to estimate k. These methods followed two dissipation-based and CPTu-based approaches. In the dissipation-based approach, k was estimated based on the interpreted t_{50}, using two empirical equations. On the other hand, in the CPTu-based approach, k was estimated using the measurements of CPTu test. These utilized methods are presented in Table 4.

Table 3. Vertical permeability, k_v, measured in the lab for three samples, from different depths.

Sample	Depth (m)	Bulk unit weight, γ (kN/m^3)	In-situ mean eff. stress (kPa)	Back pressure (kPa)	Vertical Permeability, k_v (m/sec)
FIN24-S8-S010-2.45-perm	2.39-2.50	17.9	22	10	9.16E-09
FIN24-S8-S010-3.35-perm	3.29-3.40	17.5	25	12	4.70E-10
FIN24-S8-S010-4.45-perm	4.29-4.40	17.5	29	14	2.50E-07
Average		17.6			8.67E-08

Table 4. Utilized methods to estimate permeability, k, based on two dissipation-based and CPTu-based approaches.

Approach	Equation/Value	Condition	Reference
Dissipation-based approach	$k(cm/s) = \left[\frac{1}{251 t_{50}}\right]^{1.25}$	Different types of soils	Parez & Fauriel (1988) [2]
	$k(cm/s) = \left[\frac{1}{720 t_{50}}\right]^{1.05}$	Silty sand samples	Ziaie-Moayed et al. (2009) [3]
CPTu-based approach	$k(m/s) = 10^{(0.952-3.04 I_c)}$	$1.0 \leq I_c \leq 3.27$	Robertson (2010) [1]
	$k(m/s) = 10^{(-4.52-1.37 I_c)}$	$3.27 \leq I_c \leq 4.0$	
	3E-10 ~ 3E-08	1: sensitive fine-grained [NA]	Robertson (2010) [1]
	1E-10 ~ 1E-08	2: Organic soils– clay [I_c>3.60]	
	1E-10 ~ 1E-09	3: Clay [2.95<I_c<3.60]	
	3E-09 ~ 1E-07	4: Silt mixture [2.95<I_c<3.60]	
	1E-07 ~ 1E-05	5: Sand mixture [2.95<I_c<3.60]	
	1E-05 ~ 1E-03	6: Sand [2.95<I_c<3.60]	
	1E-10 ~ 1	7: Dense sand to gravelly sand [2.95<I_c<3.60]	
	1E-08 ~ 1E-03	8: Very dense/stiff soil [2.95<I_c<3.60]	

5.5. Comparison of k estimation methods

Using the methods in Table 4, k was computed at the depths of the dissipation tests, for both dissipation- and CPTu-based approaches. For the two equations proposed by Parez and Fauriel (1988) [2] and Ziaie-Moayed et al. (2009) [3], the parameter t_{50} for dilative behavior was computed using the three aforementioned methods proposed by Sully et al. (1999) [8] and Chai et al. (2012) [9]. As we know, for the correction of t_{50} in the third method, s_u embedded in equation (5.1) is interpreted using two values of N_{kt} proposed in [12] and [26] and a single value of N_{ke} [26], as in equations (5.2) and (5.3), respectively. The computed permeability, k, results are compared in Figure 11 for all applied methods. The estimated results are also compared with the laboratory vertical permeability, k_v, results.

Jamiolkowski et al. (1985) [27] studied ranges of k_h/k_v mainly for clays, as presented in Table 5. The table was used in this study to find a rough estimate of the k_h values, using the experimental k_v measured in the lab. Since highly varved silts exist at the Finninmäki testing site, the k_h/k_v range of 3 to 15 was applied to the lab k_v measurements. This assumption was made according to the third row of Table 5, considering the soils at the testing site as 'more or less continuous permeable layers'. The sawtooth patterns of q_c, f_s, and u_2 in Figure 2 indicate the presence of varved soils at the testing site,

particularly below 2.5 m. Figure 11 compares the derived k_h values with those obtained from other methods.

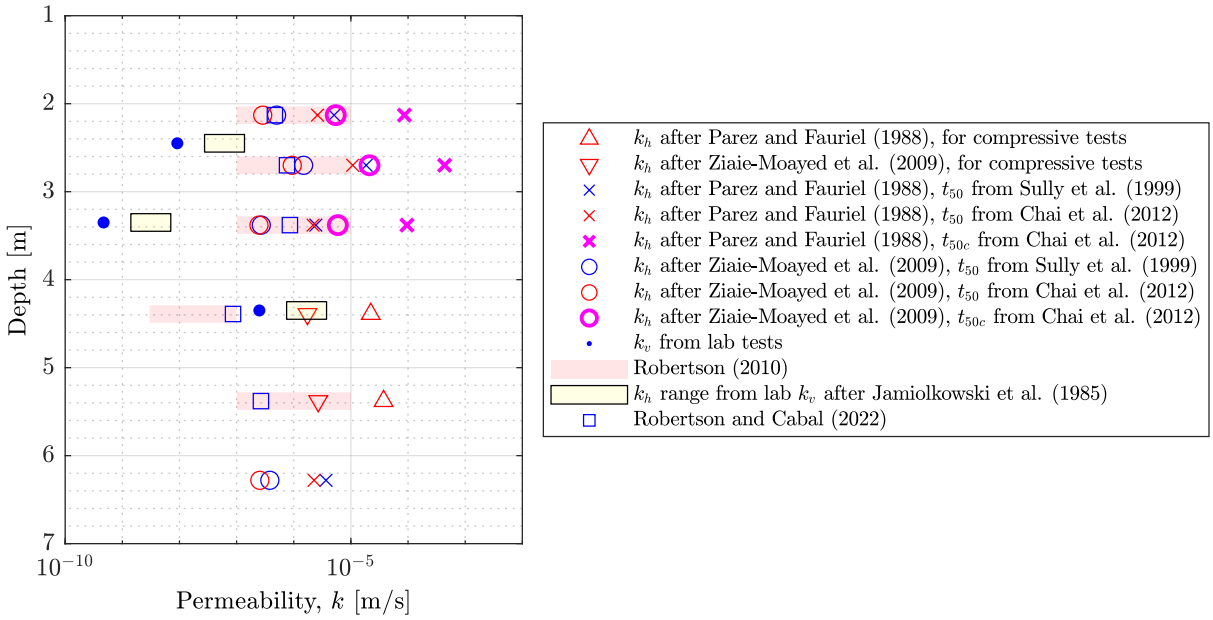

Figure 11. Comparison of different methods used to estimate permeability, k. The horizontal permeability, k_h, is estimated using the two equations proposed by Parez and Fauriel (1988) [2] and Ziaie-Moayed et al. (2009) [3], presented in Table 4. In these equations, the parameter t_{50} for dilative behavior is estimated using three methods by Sully et al. (1999) [8] and Chai et al. (2012) [9]. The permeability, k, values from two CPTu-based methods are compared herein, which are proposed by Robertson (2010) [1]. These estimated k are compared with the vertical permeability, k_v, measured in the lab. The suggested k_h/k_v ratio of 3–15 by Jamiolkowki et al. (1985) [27] is used to estimate k_h from the lab k_v tests.

Figure 11 shows a large variation among all k_h estimations. For the dissipation tests at depths of 2.13, 2.70, 3.38, 4.39, 5.38, and 6.28 m, the absolute difference between the maximum and minimum estimates of k_h –defined as $max(k_{h_i}) - min(k_{h_i})$, where k_{h_i} denotes the estimations for the dissipation test i– are 8.61E–5, 4.36E–4, 9.55E–5, 2.21E–5, 3.71E–5, and 3.41E-6 m/s, respectively, for deterministic methods. Despite this high variability, the accuracy of the k_h estimation methods were evaluated quantitatively. As presented in Table 6, $k_{h,avg}$, derived from the lab tests, was used as the benchmark for comparisons. $k_{h,avg}$ is the mid-point of the lab k_h bounds approximated using the k_h/k_v assumption of 3 to 15. The comparison was conducted using the error criterion, absolute relative error (ARE)= $\left|\frac{k_{h_i}-k_{h,avg_i}}{k_{h,avg_i}}\right|$, where k_{h_i} represents k_h estimate by each method for dissipation test i. The minimum ARE are highlighted in bold for each pairwise comparison in the table. To clarify, dissipation tests at 2.70, 3.38, and 4.39 m were compared with the lab results from 2.45, 3.35, and 4.35 m, respectively. The results indicate that the equation by Ziaie-Moayed et al. (2009) [3] presents the most accurate estimations of k_h for the two dilative-behavior tests at z = 2.45 and 3.35 m, and for the contractive-behavior test at z = 4.35 m. For dilative tests, the first t_{50} interpretation method by Chai et

al. (2012) [9] used in the quation by Ziaie-Moayed et al. (2009) [3] outperformed the other methods; although its estimations were not accurate. This finding indicates that the equation by Ziaie-Moayed et al. (2009) [3], originally proposed for sands and silty sands, performs best among the evaluated methods for the coarse silt at the Finninmäki testing site.

Table 5. Possible ranges of horizontal to vertical permeability, k_h/k_v, values for soft clays, after Jamiolkowski et al. (1985) [27].

Nature of clay	k_h/k_v
No microfabric, or only slightly developed microfabric, essentially homogeneous deposits	1.0–1.5
From fairly well to well-developed microfabric, e.g., sedimentary clays with discontinuous lenses and layers of more permeable material	2.0–4.0
Varved clays and other deposits containing embedded and more or less continuous permeable layers	3.0–15.0

Table 6. Estimated versus approximated experimental k_h measurements, based on the assumption $k_h/k_v = 3 - 15$ [27], with absolute relative error (ARE) at different depths. The $k_{h,lab}$ and estimated k_h are compared for z =2.70 vs. 2.45, 3.38 vs. 3.35, and 4.39 vs. 4.35 m, with the minimum ARE highlighted in bold. The non-deterministic CPTu-based k_h estimation method by Robertson (2010) [1] is excluded here.

Lab		Estimate of k_h			Absolute Relative Error (ARE)		
			z (m)				
z (m)	$k_{h,avg}$ *	Method	2.70	3.38	4.39	2.70	3.38	4.39
2.45	8.25E-8	PF_{cntrc} **			2.20E-5			8.88
3.35	4.23E-9	ZM_{cntrc}			1.70E-6			**0.23**
4.35	2.25E-6	PF-Sully	1.85E-5	2.44E-6		60.61	575.83	
		PF-Chai1	1.07E-5	2.18E-6		30.53	514.37	
		PF-Chai2	4.36E-4	9.57E-5		1046.91	22623.11	
		ZM-Sully	1.49E-6	2.71E-7		5.09	63.07	
		ZM-Chai1	9.41E-7	2.46E-7		**2.47**	**57.20**	
		ZM-Chai2	2.11E-5	5.91E-6		64.74	1396.16	
		Rob	7.62E-7	8.56E-7	8.66E-8	4.67	201.41	0.96

* $k_{h,avg}$ is calculated averaging the lower and upper limits of k_h calculated from the k_v reported in Table 3, based on the k_h/k_v from Table 5.

** PF, cntrc, ZM, Sully, Chai1, Chai2, Rob, stand for Parez and Fauriel (1988) [2], contractive, Ziaie-Moayed et al. (2009) [3], Sully et al. (1999) [8], Chai et al. (2012) [9]-first method without correction for t_{50}, Chai et al. (2012)-second method with correction for t_{50}, Robertson (2010) [1], respectively.

Figure 11 illustrates that, in general, the k values estimated by dissipation-based methods are higher than those estimated by CPTu-based methods. However, for dilative-behavior tests at depths of 2.13,

2.70, and 3.34 m, the deterministic CPTu-based estimations of k by Robertson (2010) [1] are almost similar to the estimations of the equation by Ziaie-Moayed et al. (2009) [3]. This similarity is not observed for the contractive-behavior tests, at depths of 4.39 and 5.38 m.

As also shown in Figure 11, k estimations are highly variable for the contractive-behavior tests. For these two contractive-behavior dissipation tests, the CPTu-based k estimates are much smaller than those estimated by the dissipation-based methods. As an example, k estimated by Robertson (2010) [1] was 8.66E–8 m/s, while Parez-Fauriel (1988) [2] and Ziaie-Moayed et al. (2009) [3] equations resulted into 2.22E-5 and 1.74E–6 m/s, respectively, which are 256 and 20 times larger.

Another interesting observation that can be traced in Figure 11 is the influence of t_{50} derivation methods on k estimations. Table 2 shows that t_{50c} calculated by the method proposed by Chai et al. (2012) [9], called Method 3, are about 95% different from t_{50} obtained from Methods 1 and 2, proposed by Sully et al. (1999) [8] and Chai et al. (2012) [9], respectively. For the largest variation in t_{50} and t_{50c}, in dilative-behavior dissipation test at depth of 3.38 m, which is 95.1%, the $t_{50_{max}}$ and $t_{50_{min}}$ are 34.03 and 1.65 seconds, derived using Methods 2 and 3, respectively. Methods 2 and 3 estimated k_h equal to 2.18E-6 and 9.57E–5 using the equation by Parez and Fauriel (1988), and equal to 2.46E–7 and 5.91E–6 using the equation by Ziaie-Moayed et al. (2009) [3], respectively. They indicate that smaller t_{50} values result into 43.9 and 24.0 times larger k_h estimates for Parez and Fauriel (1988) [2] and Ziaie-Moayed et al. (2009) [3] methods, for the depth of 3.38 m. This comparison indicates the significance of t_{50} interpretation method on the k estimation.

Figure 11 demonstrates also that the k estimates using the equation of Parez and Fauriel (1988) [2] are larger than those using the equation of Ziaie-Moayed et al. (2009) [3], at about 9 to 21 times. For dissipation test at the depth of 2.13 m, after interpreting t_{50} from the first method by Chai et al. (2012) [9], the k estimate, using the equation by Parez and Fauriel (1988) [2], was 9.09 times larger than k using the equation by Ziaie-Moayed et al. (2009) [3]. In a similar observation, for the dissipation test at the depth of 2.70 m, the k estimate using the equation by Parez and Fauriel (1988) [2] is 20.64 times larger than k using the equation by Ziaie-Moayed et al. (2009) [3], the largest difference observed in dissipation-based k estimation methods. This finding reveals the significance of the k estimation methods to derive realistic values of k.

6. Conclusions

The pore water pressure, u_2, from piezocone penetration testing (CPTu) and its dissipation with time can be correlated with the soil permeability, k. This study evaluated several handy methods to estimate k for the varved coarse silts at the Finninmäki testing site, Tampere, Finland, following the CPTu-based and dissipation-based interpretation approaches. For this purpose, a series of dissipation tests were performed at different depths, in adjunct with the CPTu and seismic CPTu tests. The estimated k was compared with the k results measured in the lab. This investigation led to the following key findings:

- In the non-plastic coarse silts studied, pore water pressure, u_2, dissipated almost completely after 100–1000 seconds. The tests can be regarded as rapid dissipation tests compared to dissipation tests in clays that may last hours for the complete dissipation of u_2.
- The three studied interpretation methods to identify t_{50} for dilative behavior dissipation tests

resulted in variable t_{50} values ranging from 31.9 to 95.1% of difference, computed as $[(t_{50,max} - t_{50,min})/t_{50,max}] \times 100$.

- The comparison of the three evaluated t_{50} interpretation methods, for each k estimation method, revealed that the calculated k can be variable, spanning 24 to 44 times for dilative-behavior dissipation tests.
- For similar t_{50} interpretation methods, using different k estimation equations led to variable k values, being about 9 to 21 times different.
- The dissipation-based methods led to smaller values of k compared to the CPTu-based k estimation methods. However, the CPTu-based method results were approximately similar to the dissipation-based method by Ziaie-Moayed et al. (2009) [3], following the first and second utilized t_{50} interpretation methods for the dilative-behavior dissipation tests. In contrast, the estimated k were more variable for the contractive-behavior dissipation tests.
- Although the evaluated dissipation- and CPTu-based k estimation methods did not result in a reasonable agreement with the lab results, it was observed that the equation by Ziaie-Moayed et al. (2009) [3] estimated k_h values closest to the lab k_h estimates at the Finninmäki testing site.

It can be concluded that there is a need to improve or develop methods to estimate k_h from the CPTu dissipation tests, both for contractive- and dilative-behavior dissipation tests, for the coarse-grained varved silts, which requires a rich database.

Author contributions

Mohammad Sadegh Farhadi: Investigation, Methodology, Software, Visualization, Writing. Eetu Pöyry: Investigation. Tim Tapani Länsivaara: Funding acquisition, Project administration, Resources, Writing - Review and Editing, Validation.

Use of AI tools declaration

The authors declare that they have not used Artificial Intelligence (AI) tools in the creation of this article.

Acknowledgments

We would like to thank Väylävirasto Oy mainly for their financial support for the project "FINCONE II". The laboratory staff of the Geotechnical lab at the Research Center TERRA, Tampere University are appreciated for their collaboration to perform the field and also lab tests, specifically Ville Kinnunen and Nuutti Vuorimies. The effort by Markus Haikola was helpful in the preliminary study of the testing site.

Conflict of interest

The authors declare that there are no conflicts of interest regarding the publication of this paper. Prof. Tim Tapani Länsivaara is the Guest Editor for AIMS Geosciences and was not involved in the editorial review or the decision to publish this article.

References

1. Robertson PK (2010) Estimating in-situ soil permeability from CPT & CPTu, In: Robertson PK, Mayne PW, Eds., *2nd international symposium on cone penetration testing,* Huntington Beach, California, USA, 535–542.
2. Parez L, and Fauriel R (1988) Le piézocône améliorations apportées à la reconnaissance des sols. *Rev Franç Géotech* 44: 13–27. https://doi.org/10.1051/geotech/1988044013
3. Ziaie-Moayed R, Naeini SA, Baziar MH (2009) Strength-flow parameters of loose silty sands from piezocone tests. *AUT J Model Simul* 41: 15–23. https://doi.org/10.22060/miscj.2009.236
4. Lech M, Marek B, Markowska-Lech K, et al. (2023) Evaluating hydraulic parameters in clays based on in situ tests. *Open Eng* 13: 20220483. https://doi.org/10.1515/eng-2022-0483
5. Robertson PK, Sully JP, Woeller DJ, et al. (1992) Estimating coefficient of consolidation from piezocone tests. *Can Geotech J* 29: 539–550. https://doi.org/10.1139/t92-061
6. Henderson E (1994) *Evaluation of the time response of pore pressure measurements.* Massachusetts Institute of Technology.
7. Hébert MC (2013) The importance of accurate pore water pressure measurements when conducting CPTu as exemplified using data collected in Christchurch following the Canterbury earthquake sequence, In: Chin CY, Eds., *19th NZGS Geotechnical Symposium*, Queenstown, New Zealand.
8. Sully JP, Robertson PK, Campanella RG, et al. (1999) An approach to evaluation of field CPTU dissipation data in overconsolidated fine-grained soils. *Can Geotech J* 36: 369–381. https://doi.org/10.1139/t98-105
9. Chai J, Daichao S, Carter JP, et al. (2012) Coefficient of consolidation from non-standard piezocone dissipation curves. *Comput Geotech* 41: 13–22. https://doi.org/10.1016/j.compgeo.2011.11.005
10. Robertson PK (2009) Interpretation of cone penetration tests—a unified approach. *Can Geotech J* 46: 1337–1355. https://doi.org/10.1139/T09-065
11. Mayne PW, Cargill E, Greig J (2023) The cone penetration test: A CPT design manual. Available from: ConeTec Group, Canada.
12. Robertson PK, Cabal K (2022) *Guide to cone penetration testing,* 7 Eds., Signal Hill, California, Gregg Drilling & Testing Inc.
13. Maanmittauslaitos kartta, 2025. Available from: `https://asiointi.maanmittauslaitos.fi/karttapaikka/?lang=en`.
14. Google Earth Pro, Version 7.3.6, 2025. Available from: `https://www.google.com/earth/`.
15. Pöyry E, Farhadi MS, Haikola M, et al. (2024) Soil plugging in small diameter tube samplers in silty soils, In: Guerra N, Fernandes NN, Ferreira C., et al. Eds., *Geotechnical Engineering Challenges to Meet Current and Emerging Needs of Society,* CRC Press, 745–749.
16. ISO 22476-1, Geotechnical investigation and testing—Field testing—Part 1: Electrical cone and piezocone penetration test, Standards from ISO are available both individually, directly through the ANSI webstore, and as part of a Standards Subscription.

17. Golestani Dariani AA, Ahmadi MM (2021) Generation and dissipation of excess pore water pressure during CPTu in clayey soils: a numerical approach. *Geotech Geol Eng* 39: 3639–3653. https://doi.org/10.1007/s10706-021-01716-z

18. Paniagua López AP, Carroll R, L'Heureux, JS, et al. (2016) Monotonic and dilatory excess pore water dissipations in silt following CPTU at variable penetration rate, In: Lehane BM, Acosta-Martínez HE, Kelly R, Eds., *Fifth International Conference on Geotechnical and Geophysical Site Characterization (ISC'5).* 5: 509–514.

19. Silva MF (2005) *Numerical and physical models of rate effects in soil penetration,* Doctoral dissertation, Cambridge University, Cambridge, UK.

20. Robertson PK (2016) Cone penetration test (CPT)-based soil behaviour type (SBT) classification system—an update. *Can Geotech J* 53: 1910–1927. https://doi.org/10.1139/cgj-2016-0044

21. Farhadi MS, Länsivaara TT, Tonni L (2022) Application of integrated Game Theory-optimization subground stratification (-IGTOSS) model to Venetian Lagoon deposits, In: Gottardi G, Tonni L, Eds., *Cone Penetration Testing 2022,* CRC Press, 394–399. https://doi.org/10.1201/9781003308829-54

22. Farhadi MS, Länsivaara TT, and L'Heureux JS, et al. (2022) Application of two novel CPTu-based stratification models, In: Gottardi G, Tonni L, Eds., *Cone Penetration Testing 2022,* CRC Press, 400–406. https://doi.org/10.1201/9781003308829-55

23. Farhadi MS, Länsivaara TT (2022) Development of an integrated game theory-optimization subground stratification model using cone penetration test (CPT) measurements. *Eng Comput* 38: 1227–1242. https://doi.org/10.1007/s00366-020-01243-0

24. Mayne PW, Peuchen J, Bouwmeester D (2010) Soil unit weight estimation from CPTs, In: Robertson PK, Mayne PW, Eds., *2nd International Symposium on Cone Penetration Testing,* Huntington Beach, CA, USA.

25. Burns SE, Mayne PW (1998) Monotonic and dilatory pore-pressure decay during piezocone tests in clay. *Can Geotech J* 35: 1063–1073.

26. Fu S, Shen Y, Jia X, et al. (2024) A novel method for estimating the undrained shear strength of marine soil based on CPTU tests. *J Mar Sci Eng* 12: 1019. https://doi.org/10.3390/jmse12061019

27. Jamiolkowki M, Ladd CC, Germaine JT, et al. (1985) New developments in field and laboratory testing of soils, In: *Proceedings of the Eleventh International Conference on Soil Mechanics and Foundation Engineering,* San Fransisco, Balkema (AA).

Supplementary

The developed code, utilized data, and the actual calculations performed for this article, can be found here: https://github.com/msf1092.